Biological Sciences/ Evolution

Dissecting historical changes of selective pressures in the evolution of human pigmentation

Xin Huang[a,b], Sijia Wang[a,c], Li Jin[a,c,1], Yungang He[a,1]

[a] Chinese Academy of Sciences Key Laboratory of Computational Biology, Chinese Academy of Sciences-Max Planck Society Partner Institute for Computational Biology, Shanghai Institutes for Biological Sciences, Shanghai, 200031, China

[b] Chinese Academy of Sciences, University of Chinese Academy of Sciences, Beijing, 100049, China

[c] State Key Laboratory of Genetic Engineering and Ministry of Education Key Laboratory of Contemporary Anthropology, Collaborative Innovation Center for Genetics and Development, School of Life Sciences, Fudan University, Shanghai, 200433, China

[1] **Corresponding authors:** lijin@fudan.edu.cn (L.J.), yunganghe@picb.ac.cn (Y.H.)

Short title: Selective pressures during different epochs

Keywords: complex trait, epistasis, human evolution, natural selection

Abstract

Human pigmentation is a highly diverse trait among populations, and has drawn particular attention from both academic and non-academic investigators for thousands of years. To explain the diversity of human pigmentation, researchers have proposed that human pigmentation is adapted for ultraviolet radiation and driven by natural selection. Although studies have detected signals of natural selection in several human pigmentation genes, none have quantitatively investigated the historical selective pressures on pigmentation genes during different epochs and thoroughly compared the differences in selective pressures between different populations. In the present study, we developed a new approach to dissect historical changes of selective pressures in a multiple population model by summarizing selective pressures on multiple genes. We collected genotype data of 16 critical human pigmentation genes from 15 public datasets, and obtained data for 3399 individuals of five representative populations from worldwide. Our new approach quantified not only a recent incremental change of selective pressure (0.68×10^{-2}/generation) in modern Europeans, but also a significant historical increase of selective pressure (1.78×10^{-2}/generation) on light pigmentation shared by all Eurasians during the out-of-Africa event. We excluded the relaxation of selective pressures, and favored diversifying selection as the single explanation for the cause of light pigmentation in Eurasians, a long-standing puzzle in the evolution of human pigmentation. Our results suggest that epistasis plays important roles in the evolution of human pigmentation, partially explaining diversifying selection on human pigmentation among populations.

Significance

The color variation of human skin, hair, and eye is affected by multiple genes with different roles. This diversity may be shaped by natural selection and adapted for ultraviolet radiation in different environments around the world, since anatomically modern human migrated out from Africa to Eurasia. Here, we developed a new approach and quantified incremental changes of selective pressures on light pigmentation not only in modern Europeans but also in proto-Eurasians. Our results support diversifying selection as the single explanation for the cause of light pigmentation in Eurasians, and suggest that epistasis might have played important roles in the evolution of human pigmentation during the out-of-Africa event.

Introduction

Human pigmentation—the color of the skin, hair, and eye—is one of the most diverse traits among populations. Its obvious diversity has attracted particular attention from both academic and non-academic investigators for thousands of years, as noted by Charles Darwin one century ago (1, p. 192) and as noticed by ancient Egyptians more than 4000 years ago (2, p. 6). Why human pigmentation diverges, however, remains a central puzzle in human biology (3). Some researchers have proposed that the diversity of human pigmentation is adapted for ultraviolet radiation (UVR) and driven by natural selection (4). Natural selection may favor dark skin for effectively absorbing sunlight and light skin for efficiently producing vitamin D. Dark skin may protect individuals against sunburn and skin cancer in low latitude areas with high UVR (4, 5), while light skin may prevent rickets amongst infants in high latitude areas with low UVR (6, 7). A better understanding of how natural selection shapes the diversity of human pigmentation could provide relevant and beneficial information for public health (4).

During the last 10 years, studies have applied statistical tests to detect signals of natural selection in several human pigmentation genes (8–18). These genes encode different proteins, including: signal regulators—ASIP, KITLG, MC1R—stimulating the melanogenic pathway; possible enhancers—BNC2, HERC2—regulating pigmentation gene expression; important enzymes—TYR, TYRP1—converting tyrosine into melanin; putative exchangers—OCA2, SLC24A4, SLC24A5, SLC45A2, TPCN2—controlling the environment within melanosomes; and an exocyst complex

unit and molecular motor—EXOC2, MYO5A—conveying vesicles and organelles within the cytoplasm (19–33). These proteins work at different stages of the melanogenic pathway, illustrating that human pigmentation is a complex trait affected by multiple genes with different roles.

Previous studies applied two groups of methods for detecting natural selection. One group of methods detects unusually long extended haplotype homozygosity (8–12, 14–16). The other group of methods identifies extreme local population differentiation (8, 9, 11–14, 16). Using both groups of methods, previous studies have been devoted to understanding the evolution of individual pigmentation genes; however, few studies have examined how multiple genes contributed to the evolution of human pigmentation. Moreover, none have quantitatively investigated the historical selective pressures of pigmentation genes during different epochs, and thoroughly compared the differences of selective pressures between different populations. To overcome these weaknesses, it is necessary to perform an extensive investigation with a creative approach.

In the present study, we extended an established method (34) to dissect historical changes of selective pressures for different epochs of human evolution. Using genetic variants from worldwide populations, we quantitatively investigated the selective pressures on human pigmentation during different stages of human evolutionary history. Our results well explain the current features of human pigmentation among representative populations. Using individual variants of pigmentation genes, we thoroughly compared the differences of selective pressures between populations. Our

98 results indicate epistasis plays an important role in the evolution of human
99 pigmentation, partially leading to diversifying selection on human pigmentation
100 among populations.
101

Results

Selection model of multiple populations. We developed a new approach for dissecting historical changes of selective pressures during different epochs of human evolutionary history. The evolutionary history of five representative human populations was simplified as a binary tree (Fig. 1). Based on our previous work (34), we measured selective pressures by selection coefficients. For a single locus, we can estimate the selection (coefficient) difference per generation between populations *i* and *j* by

$$\Delta s_{i,j} = \left[\ln\left(\frac{p_D^{(i)}}{p_A^{(i)}}\right) - \ln\left(\frac{p_D^{(j)}}{p_A^{(j)}}\right) \right] / t_{i,j}, \quad \text{(Eq. 1)}$$

where p_A and p_D are the frequencies of ancestral and derived alleles, and $t_{i,j}$ is the divergence time of populations *i* and *j*. Further, we extended Eq. 1 to estimate selection differences using multiple loci (*Materials and Methods*).

In a scenario with multiple populations, we can determine selection differences in multiple loci between paired populations by selection (coefficient) changes and durations of evolutionary stages. Then we can present selection differences between all the paired populations as an underdetermined system of equations:

$$\mathbf{d} = \mathbf{T}\boldsymbol{\delta}, \quad \text{(Eq. 2)}$$

where $\mathbf{d}$ and $\boldsymbol{\delta}$ are vectors that denote the overall selection differences of population pairs and selection changes in history, and $\mathbf{T}$ is a matrix containing durations of evolutionary stages (*Materials and Methods*).

To investigate selection changes in our demographic model (Fig. 1), we

considered four independent equations from Eq. 2, and assumed that the selection change happens in only one of the two child processes after branching occurred (*Materials and Methods*). Therefore, we can dissect the evolutionary history of human pigmentation by parameterizing and solving the non-linear equations below:

$$\begin{cases} \Delta s_{2,1} t_3 = -\delta_1 t_3 + \delta_2 t_3 \\ \Delta s_{3,1} t_1 = -\delta_1 t_3 + \delta_3 t_2 - \delta_7 t_1 + \delta_8 t_1 \\ \Delta s_{4,3} t_2 = -\delta_3 t_2 + \delta_4 t_3 + \delta_6 t_2 \\ \Delta s_{5,4} t_3 = -\delta_4 t_3 + \delta_5 t_3 \\ \delta_7 = 0 \\ \delta_1 \delta_2 = 0 \\ \delta_3 \delta_6 = 0 \\ \delta_4 \delta_5 = 0 \end{cases} . \qquad \text{(Eq. 3)}$$

Multistage selection changes of human pigmentation. To apply our new approach, we first summarized the overall selection differences (vector $\mathbf{d}$ in Eq. 2) between all the population pairs in 15 loci associated with human pigmentation (*Materials and Methods*). Figure 2 plots the overall selection differences, and Table S1 provides more details. The maximum difference (3.059×10^{-2}/generation) was observed between Europeans and West Africans, while the minimum difference (0.680×10^{-2}/generation) was observed between Europeans and Siberians. The estimated 95% confidence intervals (CIs) indicate that these selection differences were significantly deviated from zero, except for the pair of East and West Africans (Table S2). The large 95% CI of the pair of East and West Africans (between -0.139×10^{-2} and 2.768×10^{-2}/generation) was likely due to the genetic drift between East and West Africans. Our results of selection differences are consistent with differences of skin reflectance between populations (Spearman correlation coefficient $\rho = 0.95$, $p < 0.001$, Table S3),

suggesting that selective pressures on multiple genes can result in different skin colors among populations. We also note that selective pressure in Siberians was slightly stronger than that in East Asians (Fig. 2), which is consistent with the view that latitude is one of the important factors in the evolution of human pigmentation (6, 35).

We next parameterized and solved Eq. 3 to dissect the overall selection differences into multistage selection changes for different evolutionary processes. This investigation gave eight possible solutions for the multistage selection changes, any of which can fully explain the observed selection differences between the population pairs (Table 1). Further analysis suggests that solution #1 is the optimal solution in our evolutionary scenario (*Materials and Methods*). We present the sequential selection changes of solution #1 in Fig. 3. This solution indicates that the largest selection change may have occurred during the out-of-Africa event (δ_8 = 1.78 $\times$ 10^{-2}/generation, Table 1), which implies a dramatic environmental change at the first stage of the great human migration.

We then summarized all the selection changes on the evolutionary path of each population (Table S4). All the eight possible solutions exhibited the same pattern that the summarized selection changes were positive for all Eurasians since the out-of-Africa event (in the range between 0.36 $\times$ 10^{-2} and 3.33 $\times$ 10^{-2}/generation, Table S4), which indicates that light skin is favorable for all Eurasians. All the solutions suggest that the modern European lineage had the largest selective pressure on derived alleles, whereas the modern East Asian lineage experienced the smallest selective pressure of light pigmentation. From the optimal solution, our results

suggest that the modern European lineage had an incremental selection change (δ_3 = 0.68 × 10^{-2}/generation, Table 1), while the modern East Asian lineage had a decremental change (δ_5 = -1.42 × 10^{-2}/generation, Table 1), experiencing a possible relaxation of selective pressure on derived alleles. These observations are consistent with the lower skin reflectance in East Asians than in Europeans (7, Table S3).

Quantification of selection differences in individual loci. Finally, we separately quantified selection differences of the selected 31 single nucleotide polymorphisms (SNPs) to explore selection patterns of the individual loci (*Materials and Methods*). Our pilot analysis illustrates that linkage disequilibrium was generally weak between these SNPs (Fig. S1). Statistical tests suggest that most of the selection differences between populations were highly significant (Table S5). Therefore, these differences probably could not be explained by population history or the relaxation of selective pressures. Based on the selection patterns of the individual loci, we categorized the 31 selected SNPs into four groups (Fig. 4).

In the first group, all Eurasians presented directional selection on derived alleles of the SNPs (Fig. 4A). This result is consistent with the observation that reduced pigmentation occurred in most populations outside Africa. In this group, rs6119471 (*ASIP*), rs2228479 (*MC1R*), and rs885479 (*MC1R*) showed extreme selection differences between Africans and Eurasians. Among them, the selection difference of rs6119471 was ranked the second largest in our study ($\Delta s_{\text{EAS-WAF}}$ = 2.274 × 10^{-3}/generation). We note that these two genes are the major regulators upstream of the melanogenic pathway (Fig. 5). Conversely, rs4776053 (*MYO5A*) and rs4959270

(*EXOC2*) had small selection differences, suggesting their little contribution to the diversity of human pigmentation.

The second and third groups showed European- and Asian-specific selection, respectively (Fig. 4B and 4C). One notable SNP is rs1426654 (*SLC24A5*), which had the largest selection difference in our study ($\Delta s_{EUR\text{-}EAS}$ = 2.625 × 10^{-3}/generation). Previous studies reported that this SNP is under strong directional selection in Europeans (8–10, 12–14, 36). Another notable SNP is rs1800414 (*OCA2*), which had the third largest selection difference in our study ($\Delta s_{EAS\text{-}WAF}$ = 2.217 × 10^{-3}/generation). Several studies have suggested directional selection on this SNP in East Asians (15, 37, 38). These large selection differences indicate the significant contributions of these SNPs to light pigmentation in Europeans and East Asians, respectively. In addition, other SNPs in these groups support the hypothesis that recent natural selection for light pigmentation independently occurred in Europeans and Asians since their divergence. In these two groups, most of the genes work downstream of the melanogenic pathway (Fig. 5).

The last group included the remaining four SNPs (Fig. 4D), which exhibited specific selection differences between limited populations pairs. Among them, the derived allele of rs1800401 (*OCA2*) is associated with dark pigmentation (20, 21, 39). Our study indicates a rare case that the variant associated with dark pigmentation might be favored by natural selection.

Discussion

In the present study, we dissected historical changes of selective pressures by summarizing the selection differences in multiple human pigmentation genes. Our results quantify not only a recent incremental change of selective pressure (δ_3 = 0.68 × 10^{-2}/generation, Table 1) in Europeans, but also a significant historical increase of selective pressure (δ_8 = 1.78 × 10^{-2}/generation, Table 1) that favored light pigmentation in all Eurasians during the out-of-Africa event. Recent studies using ancient DNA support our observation of recent directional selection in Europeans (17, 40). Compared with these ancient DNA studies, our study has the advantage that we do not need to assume population continuity (17, 41), because our study is based on genetic data from only present-day populations. Thus, our results could provide more solid evidence of the recent directional selection in Europeans. Further, our results demonstrate independent selective pressures on light pigmentation in modern Europeans and East Asians as previous studies (12, 13, 37, 38), and a shared selective pressure that favored light pigmentation in proto-Eurasian populations. This shared selection is consistent with other studies, which revealed that *ASIP*, *BNC2*, and *KITLG* were under directional selection before the divergence of ancestral Europeans and Asians (9, 42). Unlike previous studies, we summarized selective pressures on multiple human pigmentation genes with larger sample size and more representative populations. Therefore, our results could be more relevant to the evolution of human pigmentation. Overall, our results suggest that natural selection continuously favors light pigmentation in Eurasians since the out-of-Africa event, supported by allele age

227 estimation from another study (43).

228 In addition, our results of individual loci strongly suggest that epistasis plays a
229 critical role in the evolution of human pigmentation. Most of the selected genes
230 shared by Eurasians are major regulators upstream of the melanogenic pathway (Fig.
231 5), such as *ASIP*, *KITLG*, and *MC1R* (Fig. 4A). *MC1R* encodes a
232 seven-transmembrane G-protein coupled receptor that can interact with
233 α-melanocyte-stimulating hormone (α-MSH), and switch the melanogenic pathway
234 from synthesizing the red/yellow phenomelanin to black/brown eumelanin. When
235 UVR exists, MC1R is activated by α-MSH, resulting in the synthesis of eumelanin
236 (21); α-MSH can be blocked or inhibited by agouti signaling protein (ASIP), leading
237 to the production of phenomelanin (19). Most of the remaining genes (Fig. 4B and 4C)
238 with continental-specific selection patterns work downstream of the melanogenic
239 pathway (Fig. 5). These upstream genes can regulate the expression of genes
240 downstream in the melanogenic pathway, such as *TYR*, *TYRP1*, *OCA2*, and *SLC45A2*
241 (44, 45). Published genetic association studies could support our hypothesis about the
242 role of epistasis in light pigmentation. The derived allele of rs12913832 (*HERC2*)
243 significantly increases the risk of light skin, only when individuals also carry derived
244 alleles of the upstream gene *MC1R* (46, 47). These upstream genes contributed large
245 selection differences to all Eurasians (Fig. 4A), indicating that epistasis might have
246 played an important role in the evolution of human pigmentation during the
247 out-of-Africa event.

248 Finally, our results also solve the long-standing puzzle regarding whether light

249 pigmentation in low UVR areas is caused by diversifying selection or the relaxation
250 of selective pressures (17, 48, 49). We used the statistical test that we recently
251 developed (34) to exclude the relaxation of selective pressures, and favor diversifying
252 selection as the single explanation. Before our study, multiple studies closely
253 inspected *MC1R* because its coding region has unusually higher diversity in Eurasians
254 than in Africans (9, 12, 13, 16, 50–52). These studies reached different conclusions,
255 however, either diversifying selection or the relaxation of selective pressures. The
256 relaxation of selective pressures (51) would suggest that the diversity of *MC1R*
257 variants increased in Eurasians due to the lack of selective constraints. In this scenario,
258 the genetic diversity of *MC1R* variants could be largely attributed by genetic drift. In
259 contrast, diversifying selection (50) would suggest that *MC1R* variants were under
260 directional selection in Eurasians. In this scenario, genetic drift cannot explain the
261 genetic divergence of *MC1R* between Africans and Eurasians. Our results show that
262 the divergences of rs2228479 (*MC1R*) and rs885479 (*MC1R*) between Africans and
263 Eurasians are highly significant departure from neutral evolution (Table S5).
264 Experimental evidence suggests that the derived allele of rs2228479 (*MC1R*) could
265 cause lower affinity for α-MSH than the ancestral allele (56). Another study showed
266 that the derived allele of rs885479 (*MC1R*) carries a lower risk of developing freckles
267 and severe solar lentigines than the ancestral allele in East Asians (57). These studies
268 revealed the potential roles of these *MC1R* variants in pigmentation phenotypes. In
269 addition to our results, one study reported possible diversifying selection in parts of
270 the promoter sequence of *MC1R* (58). Combining our previous results with

aforementioned experimental evidence, we suggest that diversifying selection may have occurred since the out-of-Africa event, and favored light pigmentation through epistasis.

We note that our investigation has several limitations. First, we assumed that the selection change occurs in only one of the two branching processes. This assumption is consistent with the stepping stone model (59), which is a good and simple approximation to the history of human migration. Second, we obtained eight possible solutions of historical selection changes (Table 1). Although we chose the most conservative one as the optimal solution, we cannot exclude the possibility of other solutions. All the solutions, however, show the same trend of natural selection that light pigmentation is favored in all Eurasians. This reflects the difficulty of analyzing historical selective pressures, which is a well-recognized challenge in population genetics.

To summarize, our study provides information of historical selective pressures during different epochs of the evolution of human pigmentation. The results of our analysis suggest that epistasis partially explains the diversifying selection on human pigmentation among worldwide populations. Further studies are in progress to verify our present views on the evolution of human pigmentation.

Materials and Methods

Data collection. Fifteen publicly available datasets containing genotype data from worldwide human populations were downloaded from web resources (60–74).

Data preparation. All the downloaded data were transferred to genomic coordinates using NCBI dbSNP (build 144) with the Human Reference Genome hg19. A merged dataset containing 6119 individuals and 81,364 SNPs were obtained after removing duplicate and related individuals (Table S6, S7). PLINK 1.7 (75) was used to exclude SNPs for which genotyping rates were lower than 0.99 and major allele frequencies were lower than 0.05 (--geno 0.01 --maf 0.05). SNPs in strong linkage disequilibrium were removed by applying a window of 50 SNPs advanced by 5 SNPs and an r^2 threshold of 0.02 (--indep-pairwise 50 5 0.02) in PLINK. The remaining 13,499 SNPs were used for principal components analysis (PCA). PCA was performed using SMARTPCA (version: 13050) from EIGENSOFT 6.0.1 (76, 77). After removing individuals from admixed populations and outliers (Table S8) identified by PCA, 3399 individuals (Table S9) were obtained and divided into five groups according to their geographic regions for further analysis. PCA plots (Fig. S2) showed these 3399 individuals were properly separated into different population groups.

Data imputation. Genotypes of 16 human pigmentation genes with 500-kb flanking sequences on both sides were obtained from the downloaded datasets. Haplotype inference and genotype imputation were performed on the selected genotypes using BEAGLE 4.1 with 1000 Genomes phase 3 haplotypes as the reference panel (78, 79,

Table S10). During phasing and imputation, the effective population size was assumed to be 10,000 (Ne=10000), and the other parameters were set to the default values. Forty-two SNPs were selected for analysis due to their strong association with human pigmentation in published genome-wide association studies or phenotype prediction models (Table S11). Eleven SNPs (rs1110400, rs11547464, rs12203592, rs12821256, rs1800407, rs1805005, rs1805006, rs1805007, rs1805008, rs1805009, rs74653330) were removed because of their low frequencies in our datasets after imputation (Fig. S3). Because rs12203592 (*IRF4*) was removed, 15 loci with the remaining 31 SNPs were used for further analysis.

Selection difference estimation in a single locus. The logarithm odds ratios for the selected loci were calculated and used for estimating their selection differences between populations. The estimated CIs were calculated using the imputed genotype data of 31 SNPs. Variances of genetic drift between populations (Fig. S4, Table S12) were determined using 13,499 SNPs without strong linkage disequilibrium in the merged dataset (see *Data preparation*). Details of the calculations are described elsewhere (34). Results were presented in Table S5, and visualized in heat maps (Fig. 4) using Python 3.5.1 with Matplotlib 1.4.3 through Jupyter Notebook 4.1.0 in ANACONDA 2.4.0.

Selection difference estimation in multiple loci. We extended Eq. 1 to estimate the selection difference in multiple loci. Here, we take two bi-allelic loci as an example. We can estimate the selection difference of the haplotype carrying two derived alleles between populations *i* and *j* by

333 $$\Delta s_{i,j}^{D_1D_2} = \left[\ln\left(\frac{p_{D_1D_2}^{(i)}}{p_{A_1A_2}^{(i)}} \right) - \ln\left(\frac{p_{D_1D_2}^{(j)}}{p_{A_1A_2}^{(j)}} \right) \right] / t_{i,j} ,$$

334 where $p_{A_1A_2}$ is the frequency of the haplotype carrying two ancestral alleles, $p_{D_1D_2}$
335 is the frequency of the haplotype carrying two derived alleles, and $t_{i,j}$ is the
336 divergence time between populations *i* and *j*. Assuming linkage equilibrium, we have

337 $$\begin{aligned} \Delta s_{i,j}^{D_1D_2} &= \left[\ln\left(\frac{p_{D_1D_2}^{(i)}}{p_{A_1A_2}^{(i)}} \right) - \ln\left(\frac{p_{D_1D_2}^{(j)}}{p_{A_1A_2}^{(j)}} \right) \right] / t_{i,j} \\ &= \left[\ln\left(\frac{p_{D_1}^{(i)} p_{D_2}^{(i)}}{p_{A_1}^{(i)} p_{A_2}^{(i)}} \right) - \ln\left(\frac{p_{D_1}^{(j)} p_{D_2}^{(j)}}{p_{A_1}^{(j)} p_{A_2}^{(j)}} \right) \right] / t_{i,j} \\ &= \left[\ln\left(\frac{p_{D_1}^{(i)}}{p_{A_1}^{(i)}} \right) - \ln\left(\frac{p_{D_1}^{(j)}}{p_{A_1}^{(j)}} \right) \right] / t_{i,j} + \left[\ln\left(\frac{p_{D_2}^{(i)}}{p_{A_2}^{(i)}} \right) - \ln\left(\frac{p_{D_2}^{(j)}}{p_{A_2}^{(j)}} \right) \right] / t_{i,j} \\ &= \Delta s_{i,j}^{L_1} + \Delta s_{i,j}^{L_2} \end{aligned} ,$$

338 where p_{A_1} and p_{A_2} are the frequencies of ancestral alleles in the first and second
339 loci, respectively; p_{D_1} and p_{D_2} are the frequencies of derived alleles in the first
340 and second loci, respectively; and $\Delta s_{i,j}^{L_1}$ are $\Delta s_{i,j}^{L_2}$ the selection differences between
341 populations *i* and *j* in the first and second loci, respectively. Therefore, we can obtain
342 the overall selection differences of multiple loci by summarizing estimations of
343 individual loci.

344 **Selection difference dissection in a multiple population model.** We developed an
345 approach to calculate the selection differences for different evolutionary stages using
346 our demographic model of five populations (Fig. 1). When *k* is the most recent
347 common ancestral population of *i* and *j*, we can divide $\Delta s_{i,j}$ in Eq. 1 into separate
348 terms:

349 $$\Delta s_{i,j}t_{i,j} = \left[\ln\left(\frac{p_D^{(i)}}{p_A^{(i)}}\right) - \ln\left(\frac{p_D^{(k)}}{p_A^{(k)}}\right)\right] - \left[\ln\left(\frac{p_D^{(j)}}{p_A^{(j)}}\right) - \ln\left(\frac{p_D^{(k)}}{p_A^{(k)}}\right)\right].$$

350 We can further divide the selection difference between paired populations into
351 multiple terms, if there are multiple branches between them (Fig. 1). For example,
352 using the notations and demographic model in Fig. 1, we can estimate the total
353 selection difference between Europeans and West Africans as

354 $$\Delta s_{3,1}t_1 = -\left\{\left[\ln\left(\frac{p_D^{(1)}}{p_A^{(1)}}\right) - \ln\left(\frac{p_D^{(x)}}{p_A^{(x)}}\right)\right] + \left[\ln\left(\frac{p_D^{(x)}}{p_A^{(x)}}\right) - \ln\left(\frac{p_D^{(r)}}{p_A^{(r)}}\right)\right]\right\} + \left\{\left[\ln\left(\frac{p_D^{(3)}}{p_A^{(3)}}\right) - \ln\left(\frac{p_D^{(y)}}{p_A^{(y)}}\right)\right] + \left[\ln\left(\frac{p_D^{(y)}}{p_A^{(y)}}\right) - \ln\left(\frac{p_D^{(r)}}{p_A^{(r)}}\right)\right]\right\}.$$

355 Let $s_1 = \left[\ln\left(\frac{p_D^{(1)}}{p_A^{(1)}}\right) - \ln\left(\frac{p_D^{(x)}}{p_A^{(x)}}\right)\right]/t_3$, $s_3 = \left[\ln\left(\frac{p_D^{(3)}}{p_A^{(3)}}\right) - \ln\left(\frac{p_D^{(y)}}{p_A^{(y)}}\right)\right]/t_2$,

356 $s_7 = \left[\ln\left(\frac{p_D^{(x)}}{p_A^{(x)}}\right) - \ln\left(\frac{p_D^{(r)}}{p_A^{(r)}}\right)\right]/(t_1 - t_3)$, and $s_8 = \left[\ln\left(\frac{p_D^{(y)}}{p_A^{(y)}}\right) - \ln\left(\frac{p_D^{(r)}}{p_A^{(r)}}\right)\right]/(t_1 - t_2)$, then we

357 have

358 $$\Delta s_{3,1}t_1 = -s_1t_3 + s_3t_2 - s_7(t_1 - t_3) + s_8(t_1 - t_2). \quad \text{(Eq. 4)}$$

359 Therefore, we can represent the selection difference between paired populations as a
360 combination of multistage selection coefficients. Moreover, if we let s_0 be the
361 selection coefficient of the population in the root, we can express the selection
362 coefficients of populations in different branches using s_0 plus some selection changes
363 (Fig. 1). Using the notations in Fig.1, we can rewrite Eq. 4 into

364 $$\Delta s_{3,1}t_1 = -\delta_1 t_3 + \delta_3 t_2 - \delta_7 t_1 + \delta_8 t_1.$$

365 As a result, we can write down the selection differences of all the paired populations

366 in Fig. 1 as Eq. 2, where

367 $$\mathbf{d} = \begin{pmatrix} \Delta s_{2,1}t_3 & \Delta s_{3,1}t_1 & \Delta s_{4,1}t_1 & \Delta s_{5,1}t_1 & \Delta s_{3,2}t_1 & \Delta s_{4,2}t_1 & \Delta s_{5,2}t_1 & \Delta s_{4,3}t_2 & \Delta s_{5,3}t_2 & \Delta s_{5,4}t_3 \end{pmatrix}^T$$

368 $$\boldsymbol{\delta} = \begin{pmatrix} \delta_1 & \delta_2 & \delta_3 & \delta_4 & \delta_5 & \delta_6 & \delta_7 & \delta_8 \end{pmatrix}^T,$$

369 and

370 $$\mathbf{T} = \begin{pmatrix} -t_3 & t_3 & 0 & 0 & 0 & 0 & 0 & 0 \\ -t_3 & 0 & t_2 & 0 & 0 & 0 & -t_1 & t_1 \\ -t_3 & 0 & 0 & t_3 & 0 & t_2 & -t_1 & t_1 \\ -t_3 & 0 & 0 & 0 & t_3 & t_2 & -t_1 & t_1 \\ 0 & -t_3 & t_2 & 0 & 0 & 0 & -t_1 & t_1 \\ 0 & -t_3 & 0 & t_3 & 0 & t_2 & -t_1 & t_1 \\ 0 & -t_3 & 0 & 0 & t_3 & t_2 & -t_1 & t_1 \\ 0 & 0 & -t_2 & t_3 & 0 & t_2 & 0 & 0 \\ 0 & 0 & -t_2 & 0 & t_3 & t_2 & 0 & 0 \\ 0 & 0 & 0 & -t_3 & t_3 & 0 & 0 & 0 \end{pmatrix}.$$

371 Here, the superscript *T* denotes the transpose of a vector. Because this system has
372 collinearity, we chose four independent equations, and assumed that one population
373 majorly contributes to the selection difference between any paired populations *i* and *j*
374 sharing the most recent common ancestor *k*:

375 $$\delta_i \delta_j = 0.$$

376 We also assumed $\delta_7 = 0$, because the ancestral African population before the
377 divergence of East and West Africans stayed in the same environment. Its selective
378 pressure should be the same as that of the population in the root. In other words,
379 $s_7 = s_0$. Therefore, we can transform Eq. 2 into Eq. 3 and solve it in R 3.2.0 (80) with
380 RStudio 1.0.136 (81).

Optimal solution. Under neutral evolution (NE), we considered each estimated δ as an independent random variable following a normal distribution with zero mean and σ^2 variance. For each solution with four variables, the summation below follows a chi-square distribution with four degrees of freedom:

$$\frac{1}{\sigma^2}\sum_i \delta_i^2 \sim \chi^2(4).$$

Therefore, we have $\Pr(|\boldsymbol{\delta}|^2 > |\boldsymbol{\delta}_a|^2 \mid NE) \geq \Pr(|\boldsymbol{\delta}|^2 > |\boldsymbol{\delta}_b|^2 \mid NE)$, if $|\boldsymbol{\delta}_a|^2 \leq |\boldsymbol{\delta}_b|^2$ for solutions *a* and *b*. In other words, we can choose the most conservative solution with the least deviation from neutral evolution using a probabilistic approach.

Acknowledgements

This work was supported by grants from National Natural Science Foundation of China (91331109 to Y.H.; 31271338 and 31330038 to L.J.; 31322030 and 91331108 to S.W.). Y.H. is also grateful for support from the SA-SIBS scholarship program and the Youth Innovation Promotion Association of Chinese Academy of Science (2012216). L.J. was also supported by the Shanghai Leading Academic Discipline Project (B111) and the Center for Evolutionary Biology at Fudan University. S.W. was also awarded by the National Thousand Young Talents Award, the Max Planck-CAS Paul Gerson Unna Independent Research Group Leadership Award, and open projects from the State Key Laboratory of Genetic Engineering at Fudan University. X.H. is grateful to Yuchen Wang for helpful discussion on data preparation, and to Dr. Minxian Wang for helpful discussion on data imputation and comments for the manuscript. We thank anonymous reviewers for comments that improved the study and the manuscript. The authors declare no conflict of interest.

Author Contributions

Y.H. designed the study. X.H. and Y.H. developed the model, analyzed the data, and wrote the manuscript. L.J. and S.W. revised the manuscript. L.J. and Y.H. jointly supervised the study.

References

1. Darwin C (1889) *The Descent of Man, and Selection in Relation to Sex*. (Appleton and Company, New York).

2. Norton HL (2005) Human skin pigmentation variation: a phenotypic, genotypic and evolutionary perspective. Ph.D. Dissertation, Pennsylvania State University. Retrieved from https://etda.libraries.psu.edu/catalog/6658. Last visited date: 2017-02-11.

3. Rees JL, Harding RM (2012) Understanding the evolution of human pigmentation: recent contributions from population genetics. *J Invest Dermatol* 132(3):846–853.

4. Parra EJ (2007) Human pigmentation variation: evolution, genetic basis, and implications for public health. *Am J Phys Anthropol* Suppl 45:85–105.

5. Greaves M (2014) Was skin cancer a selective force for black pigmentation in early hominin evolution? *P R Soc B* 281(1781):20132055.

6. Loomis WF (1967) Skin-pigment regulation of vitamin-D biosynthesis in man. *Science* 157(3788):501–506.

7. Jablonski NG, Chaplin G (2000) The evolution of human skin coloration. *J Hum Evol* 39(1):57–106.

8. Izagirre N, García I, Junquera C, de la Rúa C, Alonso S (2006) A scan for signatures of positive selection in candidate loci for skin pigmentation in humans. *Mol Biol Evol* 23(9):1697–1706.

9. McEvoy B, Beleza S, Shriver MD. (2006) The genetic architecture of normal variation in human pigmentation: an evolutionary perspective and model. *Hum Mol Genet* 15(Spec No 2):R176–R181.

10. Voight BF, Kudaravalli S, Wen X, Pritchard JK (2006) A map of recent positive selection in the human genome. *PLoS Biol* 4(3):e72.

11. Lao O, de Gruijter JM, van Duijin K, Navarro A, Kayser M (2007) Signatures of positive selection in genes associated with human skin pigmentation as revealed from analyses of single nucleotide polymorphisms. *Ann Hum Genet* 71(3):354–369.

12. Myles S, Somel M, Tang K, Kelso J, Stoneking M (2007) Identifying genes underlying skin pigmentation differences among human populations. *Hum Genet* 120(5):613–621.

13. Norton HL, et al. (2007) Genetic evidence for the convergent evolution of light skin in Europeans and East Asians. *Mol Biol Evol* 24(3):710–722.

14. Pickrell J, et al. (2009) Signals of recent positive selection in a worldwide sample of human populations. *Genome Res* 19(5):826–837.

15. Donnelly MP, et al. (2012) A global view of the *OCA2-HERC2* region and pigmentation. *Hum Genet* 131(5):683–696.

16. Hider JL, et al. (2013) Exploring signatures of positive selection in pigmentation candidate genes in populations of East Asian ancestry. *BMC Evol Biol* 13:150.

448 17. Wilde S, et al. (2014) Direct evidence for positive selection of skin, hair, and eye
449 pigmentation in Europeans during the last 5,000 y. *Proc Natl Acad Sci USA*
450 111(13):4832–4837.

451 18. Field Y, et al. (2016) Detection of human adaptation during the past 2000 years.
452 *Science* 354(6313):760–764.

453 19. Abdel-Malek ZA, et al. (2001) The melanocortin 1 receptor is the principal
454 mediator of the effects of agouti signaling protein on mammalian melanocytes. *J*
455 *Cell Biol* 114(5):1019–1024.

456 20. Rebbeck TR, et al. (2002) *P* gene as an inherited biomarker of human eye color.
457 *Cancer Epidem Biomar* 11(8):782–784.

458 21. Duffy DL, et al. (2004) Interactive effects of MC1R and OCA2 on melanoma risk
459 phenotypes. *Hum Mol Genet* 13(4):447–461.

460 22. Duffy DL, et al. (2007) A three-single-nucleotide polymorphism haplotype in
461 intron 1 of *OCA2* explains most human eye-color variation. *Am J Hum Genet*
462 80(2):241–252.

463 23. Graf J, Hodgson R, van Daal A (2005) Single nucleotide polymorphisms in the
464 *MATP* gene are associated with normal human pigmentation variation. *Hum Mutat*
465 25(3):278–284.

466 24. Sulem P, et al. (2007) Genetic determinants of hair, eye and skin pigmentation in
467 Europeans. *Nat Genet* 39(12):1443–1452.

468 25. Sulem P, et al. (2008) Two newly identified genetic determinants of pigmentation
469 in Europeans. *Nat Genet* 40(7):835–837.

470 26. Anno S, Abe T, Yamamoto T (2008) Interactions between SNP alleles at multiple
471 loci contribute to skin color differences between Caucasoid and Mongoloid
472 subjects. *Int J Biol Sci* 4(2):81–86.

473 27. Han J, et al. (2008) A genome-wide association study identifies novel alleles
474 associated with hair color and skin pigmentation. *PLoS Genet* 4(5):e1000074.

475 28. Ito S, Wakamatsu K (2008) Chemistry of mixed melanogenesis - pivotal roles of
476 dopaquinone. *Photochem Photobiol* 84(3):582–592.

477 29. Kayser M, et al. (2008) Three genome-wide association studies and a linkage
478 analysis identify *HERC2* as a human iris color gene. *Am J Hum Genet*
479 82(2):411–423.

480 30. Sturm RA, Duffy DL (2012) Human pigmentation genes under environmental
481 selection. *Genome Biol* 13(9):248.

482 31. Visser M, Kayser M, Palstra R (2012) *HERC2* rs12913832 modulates human
483 pigmentation by attenuating chromatin-loop formation between a long-range
484 enhance and the *OCA2* promoter. *Genome Res* 22(3):446–455.

485 32. Visser M, Palstra R, Kayser M (2014) Human skin color is influenced by an
486 intergenic DNA polymorphism regulating transcription of the nearly *BNC2*
487 pigmentation gene. *Hum Mol Genet* 23(21):5750–5762.

488 33. Guenther CA, Tasic B, Luo L, Bedell MA, Kingsley DM (2014) A molecular basis
489 for classic blond hair color in Europeans. *Nat Genet* 46(7):748–754.

490 34. He Y, et al. (2015) A probabilistic method for testing and estimating selection
491 differences between populations. *Genome Res* 25(12):1903–1909.

492 35. Jablonski NG, Chaplin G (2010) Human skin pigmentation as an adaptation to UV
493 radiation. *Proc Natl Acad Sci USA* 107(Suppl 2):8962–8968.

494 36. Lamason RL, et al. (2005) SLC24A5, a putative cation exchanger, affects
495 pigmentation in zebrafish and humans. *Science* 310(5755):1782–1786.

496 37. Edwards M, et al. (2010) Association of the *OCA2* polymorphism His615Arg with
497 melanin content in East Asian Populations: further evidence of convergent
498 evolution of skin pigmentation. *PLoS Genet* 6(3):e1000867.

499 38. Yang Z, et al. (2016) A genetic mechanism for convergent skin lightening during
500 recent human evolution. *Mol Biol Evol* 33(5):1177–1187.

501 39. Jannot AS, et al. (2005) Allele variations in the *OCA2* gene (pink-eyed-dilution
502 locus) are associated with genetic susceptibility to melanoma. *Eur J Hum Genet*
503 13(8):913–920.

504 40. Mathieson I, et al. (2015) Genome-wide patterns of selection in 230 ancient
505 Eurasians. *Nature* 528(7583):499–503.

506 41. Slatkin M, Racimo F (2016) Ancient DNA and human history. *Proc Natl Acad Sci*
507 *USA* 113(23):6380–6387.

508 42. Beleza S, et al. (2013) The timing of pigmentation lightening in Europeans. *Mol*
509 *Biol Evol* 30(1):24–35.

510 43. Nakagome S, et al. (2016) Estimating the ages of selection signals from different
511 epochs in human history. *Mol Biol Evol* 33(3):657–669.

512 44. Vachtenheim J, Borovanský J (2010) "Transcription physiology" of pigment
513 formation in melanocytes: central role of MITF. *Exp Dermatol* 19(7):617–627.

514 45. San-Jose LM, et al. (2017) *MC1R* variants affect the expression of melanocortin
515 and melanogenic genes and the association between melanocortin genes and
516 coloration. *Mol Ecol* 26(1):259–276.

517 46. Branicki W, Brudnik U, Wojas-Pelc A (2009) Interactions between *HERC2*, *OCA2*
518 and *MC1R* may influence human pigmentation phenotype. *Ann Hum Genet*
519 73(2):160–170.

520 47. Pośpiech E, et al. (2014) The common occurrence of epistasis in the determination
521 of human pigmentation and its impact on DNA-based pigmentation phenotype
522 prediction. *Forensic Sci Int Gen* 11:64–72.

523 48. Rees JL (2003) Genetics of hair and skin color. *Annu Rev Genet* 37:67–90.

524 49. Harris EE, Meyer D (2006) The molecular signature of selection underlying
525 human adaptations. *Am J Phys Anthropol* Suppl 43:89–130.

526 50. Rana BK, et al. (1999) High polymorphism at the human melanocortin 1 receptor
527 locus. *Genetics* 151(4):1547–1557.

528 51. Harding RM, et al. (2000) Evidence for variable selective pressures at MC1R. *Am*
529 *J Hum Genet* 66(4):1351–1361.

530 52. Martínez-Cadenas C, et al. (2013) Simultaneous purifying selection on the
531 ancestral *MC1R* allele and positive selection on the melanoma-risk allele V60L in
532 south Europeans. *Mol Biol Evol* 30(12):2654–2665.

533 53. Wasmeier C, Hume AN, Bolasco G, Seabra MC (2008) Melanosomes at a glance.
534 *J Cell Sci* 121(24):3995–3999.

535 54. Valencia JC, Hearing VJ (2012) The role of glycosylation in the control of
536 processing and cellular transport of the functional amyloid PMEL17.
537 *Glycosylation*, ed. Petrescu (In Tech, Rijeka). Chapter 15.

538 55. Wu B, Guo W (2015) The exocyst at a glance. *J Cell Sci* 128(16):2957–2964.

539 56. Xu X, Thörnwall M, Lundin L, Chhajlani V (1996) Val92Met variant of the
540 melanocyte stimulating hormone receptor gene. *Nat Genet* 14(4):384.

541 57. Motokawa T, Kato T, Hashimoto Y, Katagiri T (2007) Effect of Val92Met and
542 Arg163Gln variants of the *MC1R* gene on freckles and solar lentigines in Japanese.
543 *Pigment Cell Res* 20(2):140–143.

544 58. Makova KD, Ramsay M, Jenkins T, Li WH (2001) Human DNA sequence
545 variation in a 6.6-kb region containing the melanocortin 1 receptor promoter.
546 *Genetics* 158(3):1253–1268.

547 59. Kimura M, Weiss GH (1964) The stepping stone model of population structure

548 and the decrease of genetic correlation with distance. *Genetics* 49(4):561–576.

549 60. Li JZ, et al. (2008) Worldwide human relationships inferred from genome-wide
550 patterns of variation. *Science* 319(5866):1100–1104.

551 61. Teo YY, et al. (2009) Singapore genome variation project: a haplotype map of
552 three Southeast Asian populations. *Genome Res* 19(11):2154–2162.

553 62. The 1000 Genomes Project Consortium (2010) A map of human genome variation
554 from population-scale sequencing. *Nature* 467(7319):1061–1073.

555 63. The International HapMap 3 Consortium (2010) Integrating common and rare
556 genetic variation in diverse human populations. *Nature* 467(7311):52–58.

557 64. Behar DM, et al. (2010) The genome-wide structure of the Jewish people. *Nature*
558 466(7303):238–242.

559 65. Rasmussen M, et al. (2010) Ancient human genome sequence of an extinct
560 Palaeo-Eskimo. *Nature* 463(7282):757–762.

561 66. Metspalu M, et al. (2011) Shared and unique components of human population
562 structure and genome-wide signals of positive selection in South Asia. *Am J Hum*
563 *Genet* 89(6):731–744.

564 67. Pagani L, et al. (2012) Ethiopian genetic diversity reveals linguistic stratification
565 and complex influences on the Ethiopian gene pool. *Am J Hum Genet*
566 91(1):83–96.

567 68. Yunusbayev B, et al. (2012) The Caucasus as an asymmetric semipermeable

568 barrier to ancient human migrations. *Mol Biol Evol* 29(1):359–365.

569 69. Yunusbayev B, et al. 2015. The genetic legacy of the expansion of
570 Turkic-speaking nomads across Eurasia. *PLoS Genet* 11(4):e1005068.

571 70. Cristofaro JD, et al. (2013) Afghan Hindu Kush: where Eurasian sub-continent
572 gene flows converge. *PLoS One* 8(10):e76748.

573 71. Fedorova SA, et al. (2013) Autosomal and uniparental portraits of the naive
574 populations of Sakha (Yakutia): implications for the peopling of Northeast Eurasia.
575 *BMC Evol Biol* 13:127.

576 72. Xing J, et al. (2013) Genomic analysis of natural selection and phenotypic
577 variation in high-altitude Mongolians. *PLoS Genet* 9(7):e1003634.

578 73. Kovacevic L, et al. (2014) Standing at the gateway to Europe - the genetic
579 structure of Western Balkan populations based on autosomal and haploid markers.
580 *PLoS One* 9(8):e105090.

581 74. Raghavan M, et al. (2014) Upper Paleolithic Siberian genome reveals dual
582 ancestry of Native Americans. *Nature* 505(7481):87–91.

583 75. Purcell S, et al. (2007) PLINK: a toolset for whole-genome association and
584 population-based linkage analysis. *Am J Hum Genet* 81(3):559–575.

585 76. Patterson N, Price AL, Reich D (2006) Population structure and eigenanalysis.
586 *PLoS Genet* 2(12):e190.

587 77. Price AL, et al. (2006) Principal components analysis corrects for stratification in

588 genome-wide association studies. *Nat Genet* 38(8):904–909.

589 78. Browning SR, Browning BL (2007) Rapid and accurate haplotype phasing and
590 missing data inference for whole genome association studies by use of localized
591 haplotype clustering. *Am J Hum Genet* 81(5):1084–1097.

592 79. Browning BL, Browning SR (2016) Genotype imputation with millions of
593 reference samples. *Am J Hum Genet* 98(1):116–126.

594 80. R Core Team (2015) R: A language and environment for statistical computing. R
595 Foundation for Statistical Computing, Vienna, Austria. URL:
596 http://www.R-project.org/.

597 81. RStudio Team (2016) RStudio: Integrated development for R. RStudio, Inc.,
598 Boston, MA. URL: http://www.rstudio.com/.
599

Figure Legends

Fig. 1. Modeling selective pressures with multiple population phylogeny. We modeled the evolutionary history of five representative human populations as a binary tree. The details of demographic events were ignored. Here, s_i (i = 0, 1, ..., 8) denotes the selection coefficient of the i-th epoch. δ_i (i = 1, 2, ..., 8) denotes the selection change of the i-th epoch, and can be obtained by estimating selection differences between paired populations. The numbers on the branches indicate different epochs. In the present study, we assumed that the divergence time of separation between Africans and Eurasians was ~3600 generations ago; the divergence time of separation between Europeans and Asians was ~3000 generations ago; the divergence time of separation between Siberians and East Asians was ~2000 generations ago; and the divergence time of separation between East and West Africans was ~2000 generations ago.

Fig. 2. The overall selection differences in multiple loci between populations. We summarized the overall selection differences in 15 loci for paired representative populations using genotype data from 15 public datasets. Red color (positive numbers) indicates selective pressures of populations in rows are larger than those in columns; blue color (negative numbers) indicates selective pressures of populations in rows are smaller than those in columns. Populations are abbreviated as follows: WAF, West Africans; EAF, East Africans; EUR, Europeans; SIB, Siberians; EAS, East Asians.

Fig. 3. Historical changes of selective pressures on human pigmentation during

different epochs of human migration. We determined historical changes of selective pressures on human pigmentation during different epochs by solving the non-linear equations developed in this study. The most conservative solution was chosen to represent the possible historical selection on the world map. We observed not only a recent incremental change of selective pressure in modern Europeans, but also a significant historical increase of selective pressure on light pigmentation in all Eurasians during the out-of-Africa event. Here, s_0 is the selection coefficient of the ancestral population for all modern human populations. The numbers are the selection changes ($\times 10^{-2}$/generation) during different epochs. Zero changes are ignored. The arrows indicate the direction of human migration, and their color gradient indicates the trends of human skin color.

Fig. 4. Selection differences in individual loci between populations. We used Eq. 1 to quantify the selection differences of 31 SNPs associated with human pigmentation, and categorized them into four kinds of selection patterns: (A) Eurasian-shared pattern; (B) European-specific pattern; (C) Asian-specific pattern; and (D) Other. Red color (positive numbers) indicates selective pressures of populations in rows are larger than those in columns; blue color (negative numbers) indicates selective pressures of populations in rows are smaller than those in columns. All alleles are in the forward strand of the Human Reference Genome, and the arrows indicate substitutions from ancestral to derived alleles. Populations are abbreviated as follows: 1, West Africans; 2, East Africans; 3, Europeans; 4, Siberians; 5, East Asians.

Fig. 5. Human pigmentation genes under different population-specific selection

643 **in the melanogenic pathway.** We placed human pigmentation genes affected by
644 population-specific selection into the melanogenic pathway. Two critical genes, *ASIP*
645 and *MC1R*, are the major regulators upstream of the melanogenic pathway. The
646 largest selection differences of these two genes were between Africans and Eurasians,
647 indicating that epistasis plays important roles in the evolution of human pigmentation.
648 Most of the remaining genes are downstream of the melanogenic pathway. The
649 melanogenic pathway is based on previous publications (4, 30–32, 53–55). The
650 arrows indicate the direction of the melanogenic pathway.
651

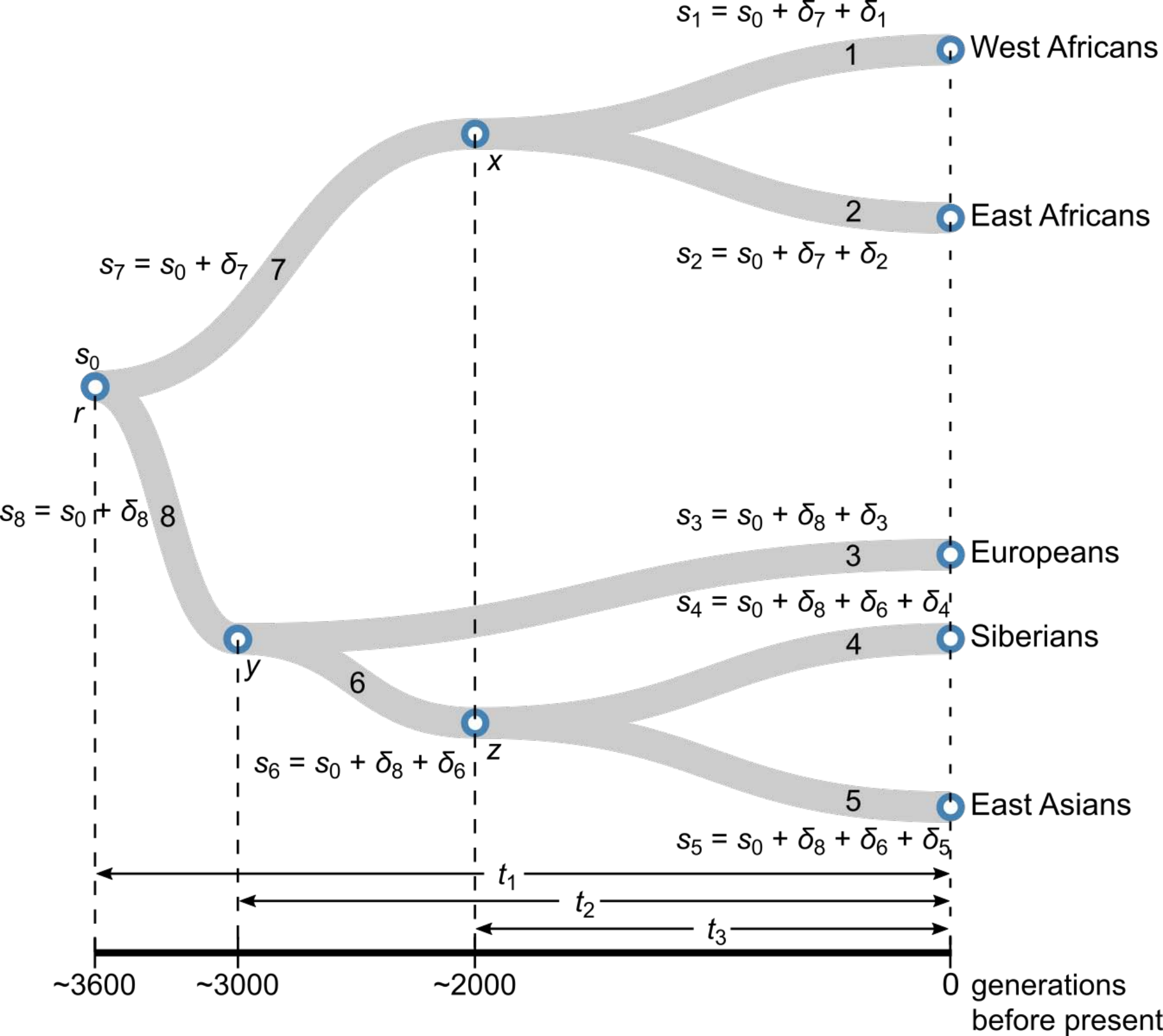
$s_1 = s_0 + \delta_7 + \delta_1$
1
West Africans
x
2
East Africans
$s_2 = s_0 + \delta_7 + \delta_2$
$s_7 = s_0 + \delta_7$
7
s_0
r
$s_8 = s_0 + \delta_8$
8
$s_3 = s_0 + \delta_8 + \delta_3$
3
Europeans
$s_4 = s_0 + \delta_8 + \delta_6 + \delta_4$
4
Siberians
y
6
z
$s_6 = s_0 + \delta_8 + \delta_6$
5
East Asians
$s_5 = s_0 + \delta_8 + \delta_6 + \delta_5$
t_1
t_2
t_3
~3600
~3000
~2000
0
generations
before present

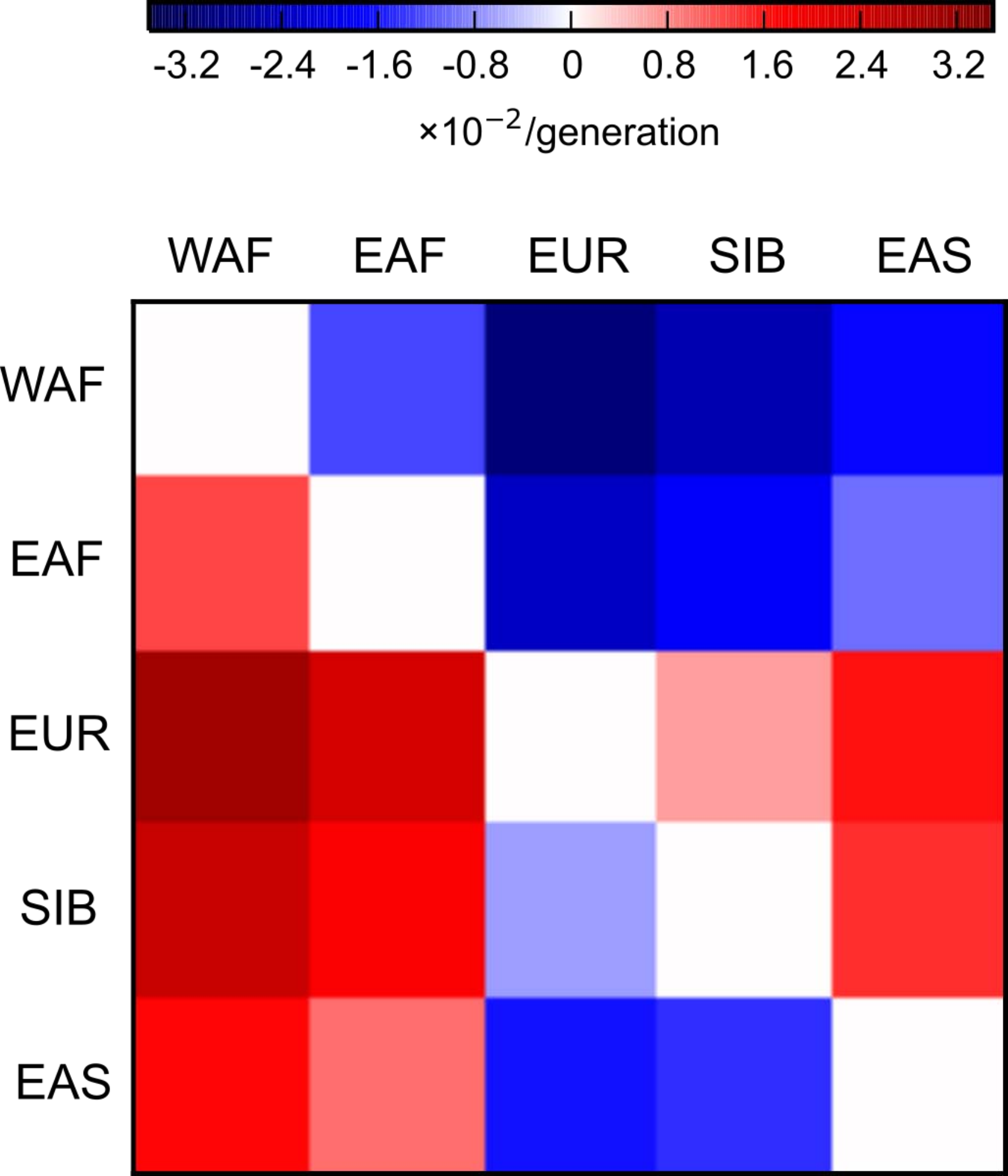
-3.2
-2.4
-1.6
-0.8
0
0.8
1.6
2.4
3.2
×10−2/generation
WAF
EAF
EUR
SIB
EAS
WAF
EAF
EUR
SIB
EAS

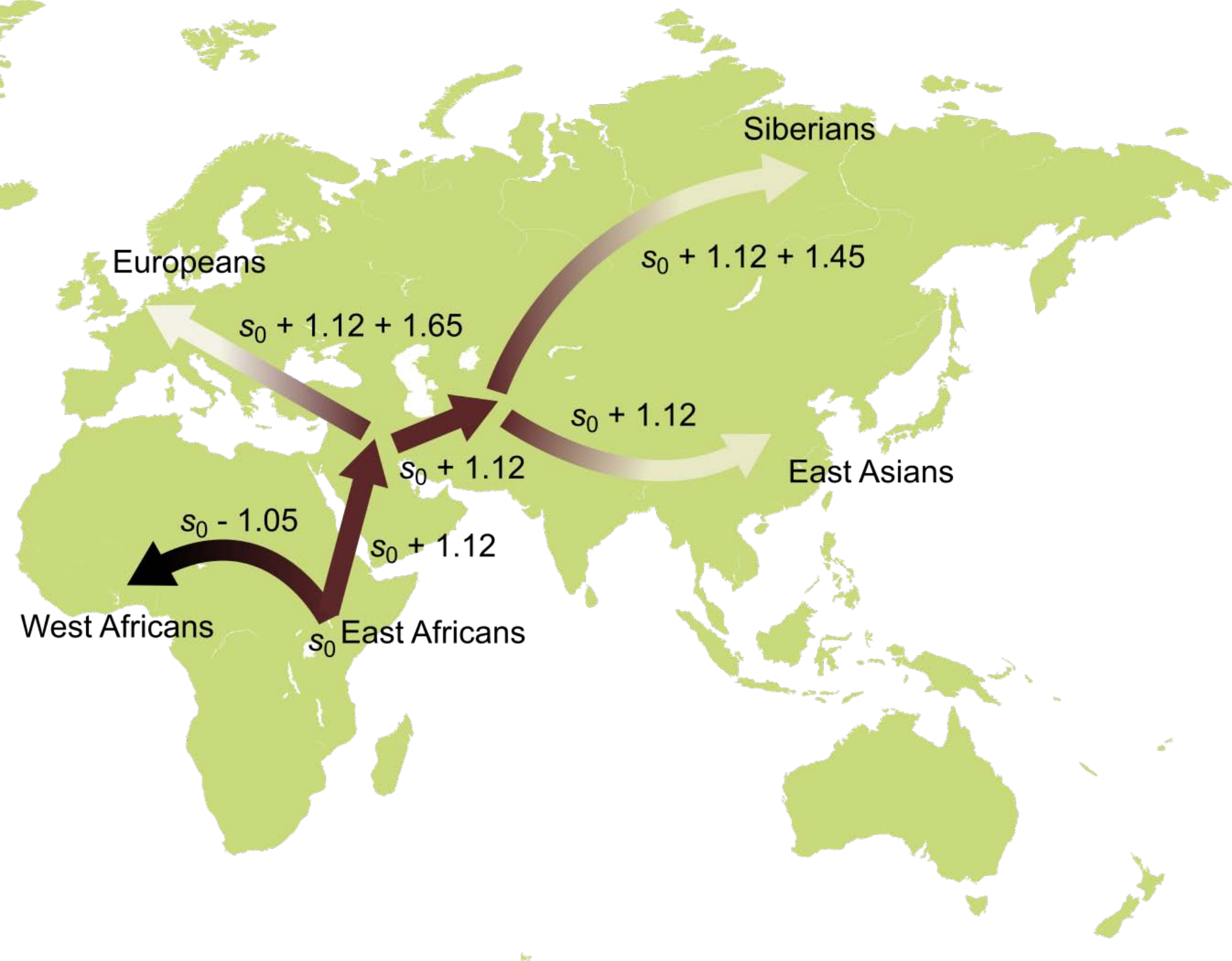
Siberians
Europeans
s_0 + 1.12 + 1.45
s_0 + 1.12 + 1.65
s_0 + 1.12
East Asians
s_0 + 1.12
s_0 - 1.05
s_0 + 1.12
West Africans
s_0 East Africans

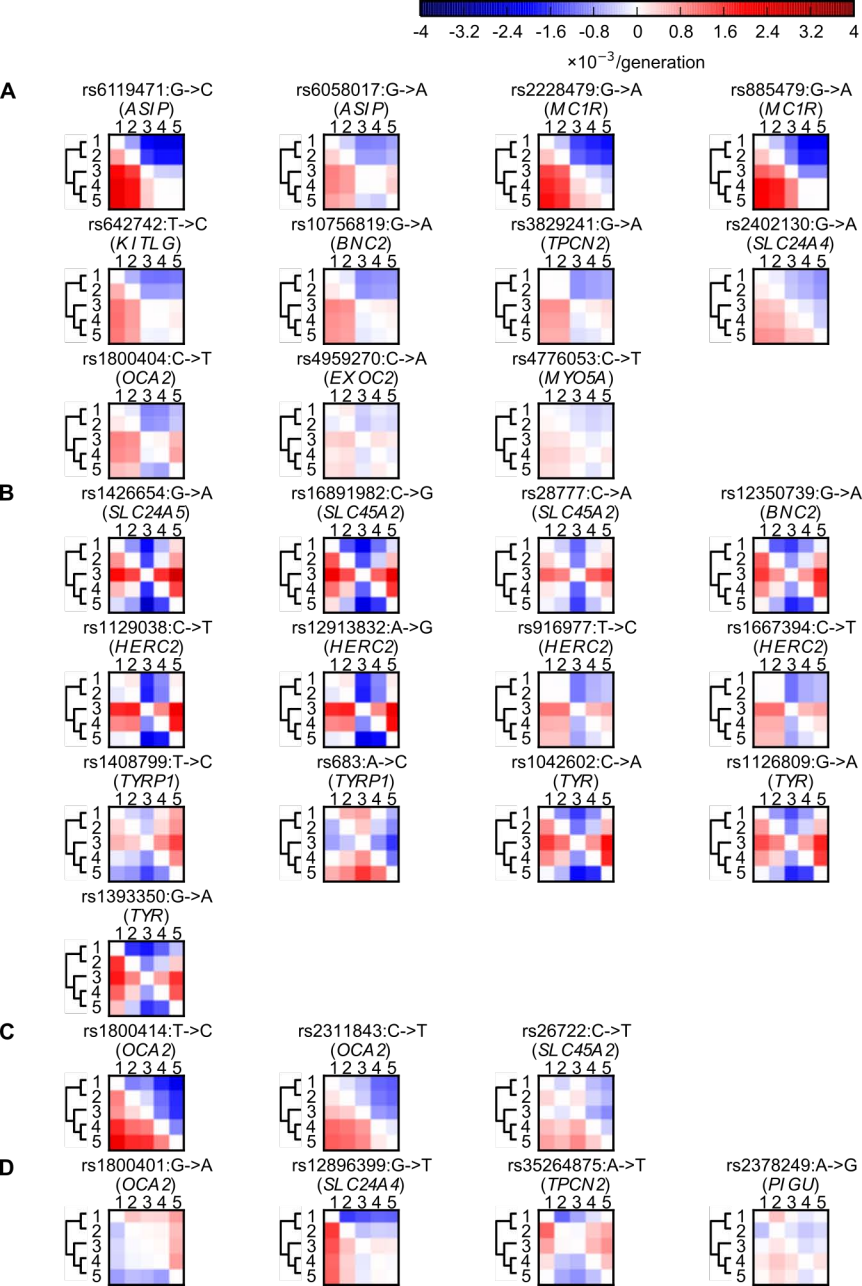
-4 -3.2 -2.4 -1.6 -0.8 0 0.8 1.6 2.4 3.2 4
×10−3/generation
A
rs6119471:G->C (ASIP)
rs6058017:G->A (ASIP)
rs2228479:G->A (MC1R)
rs885479:G->A (MC1R)
rs642742:T->C (KITLG)
rs10756819:G->A (BNC2)
rs3829241:G->A (TPCN2)
rs2402130:G->A (SLC24A4)
rs1800404:C->T (OCA2)
rs4959270:C->A (EXOC2)
rs4776053:C->T (MYO5A)
B
rs1426654:G->A (SLC24A5)
rs16891982:C->G (SLC45A2)
rs28777:C->A (SLC45A2)
rs12350739:G->A (BNC2)
rs1129038:C->T (HERC2)
rs12913832:A->G (HERC2)
rs916977:T->C (HERC2)
rs1667394:C->T (HERC2)
rs1408799:T->C (TYRP1)
rs683:A->C (TYRP1)
rs1042602:C->A (TYR)
rs1126809:G->A (TYR)
rs1393350:G->A (TYR)
C
rs1800414:T->C (OCA2)
rs2311843:C->T (OCA2)
rs26722:C->T (SLC45A2)
D
rs1800401:G->A (OCA2)
rs12896399:G->T (SLC24A4)
rs35264875:A->T (TPCN2)
rs2378249:A->G (PIGU)
1 2 3 4 5

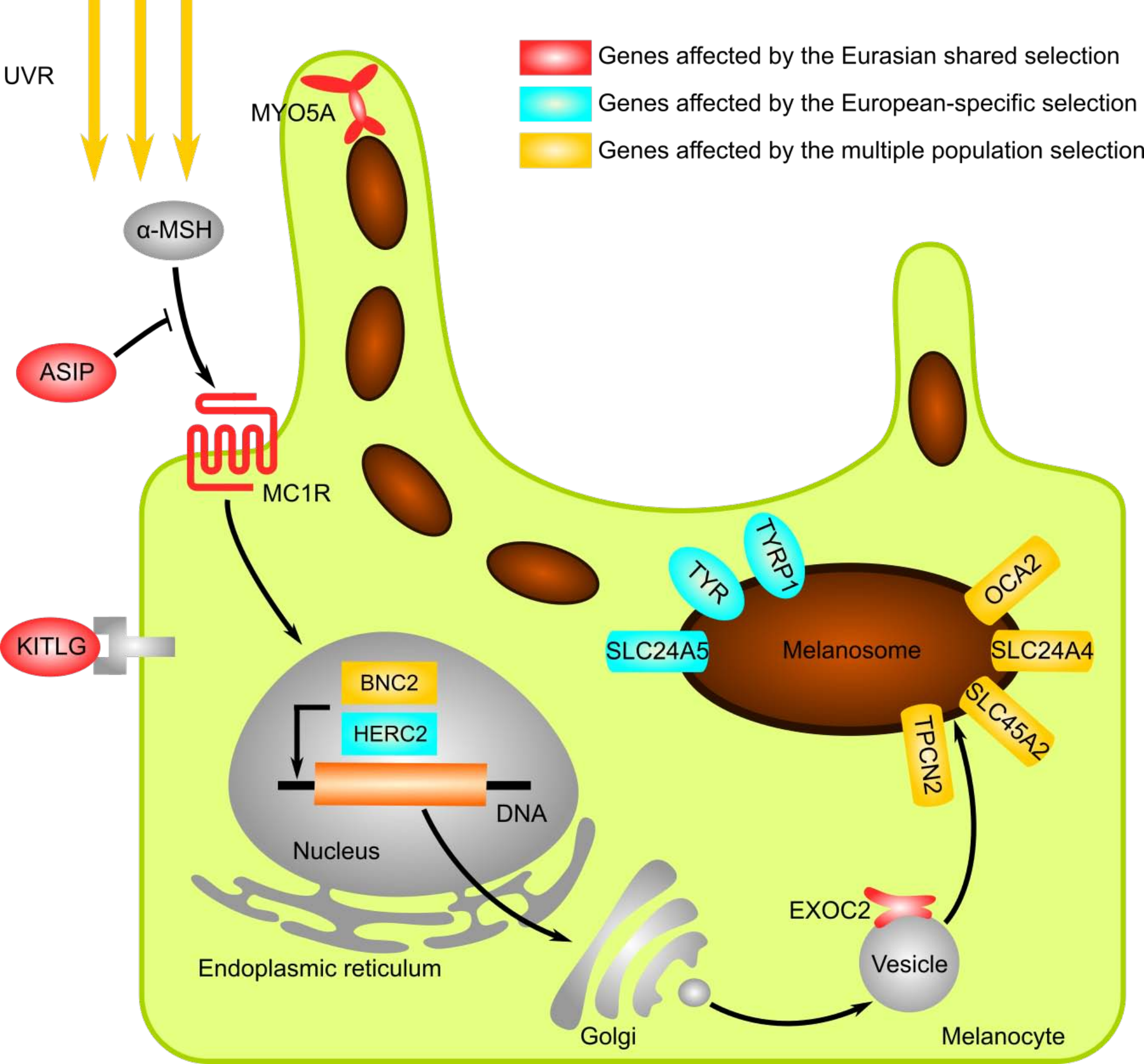
Genes affected by the Eurasian shared selection
Genes affected by the European-specific selection
Genes affected by the multiple population selection
UVR
MYO5A
α-MSH
ASIP
MC1R
KITLG
BNC2
HERC2
DNA
Nucleus
Endoplasmic reticulum
Golgi
TYR
TYRP1
OCA2
SLC24A5
Melanosome
SLC24A4
SLC45A2
TPCN2
EXOC2
Vesicle
Melanocyte

Table 1. Solutions of historical selection (coefficient) changes during different epochs ($\times 10^{-2}$/generation).

Solution	δ_1	δ_2	δ_3	δ_4	δ_5	δ_6	δ_7	δ_8
#1	-1.28	0	0.68	0	-1.42	0	0	1.78
#2	-1.28	0	1.63	1.42	0	0	0	0.99
#3	-1.28	0	0	0	-1.42	-0.68	0	2.35
#4	-1.28	0	0	1.42	0	-1.63	0	2.35
#5	0	1.28	0	0	-1.42	-0.68	0	3.06
#6	0	1.28	0	1.42	0	-1.63	0	3.06
#7	0	1.28	0.68	0	-1.42	0	0	2.49
#8	0	1.28	1.63	1.42	0	0	0	1.70

We applied our new approach to dissect historical changes of selective pressures in a multiple population model by summarizing selective pressures on multiple human pigmentation genes. Here, δ_i (i = 1, 2, ..., 8) denotes the selection change of the i-th epoch, as shown in Fig. 1. A positive change indicates a stronger directional selection on derived alleles than before; a negative change suggests a weaker positive selection on derived alleles than before. Further, we chose solution #1 as the most conservative solution using a probabilistic approach.